SOIL ECOLOGY LETTERS

SEL

RESEARCH ARTICLE

Volume 6 / Issue 4 / 240233 / 2024

https://doi.org/10.1007/s42832-024-0233-7

Hg-mining-induced soil pollution by potentially toxic metal(loid)s presents a potential environmental risk and threat to human health: A global meta-analysis

Li Chen[1,2], Xiaosan Luo[3], Haoran He[1,2], Ting Duan[4], Ying Zhou[5], Lequn Yang[5], Yi Zeng[1,2], Hansong Chen[2], Linchuan Fang[1,2,*]

1 Key Laboratory of Green Utilization of Critical Non-metallic Mineral Resources, Ministry of Education, Wuhan University of Technology, Wuhan 430070, China

2 College of Natural Resources and Environment, Northwest A & F University, Yangling 712100, China

3 International Center for Ecology, Meteorology, and Environment, School of Applied Meteorology, Nanjing University of Information Science & Technology, Nanjing 210044, China

4 School of Agriculture, Ningxia University, Yinchuan 750000, China

5 College of Environment and Resource, Xichang University, Xichang 615000, China

* Corresponding author. E-mail: flinc629@hotmail.com (L. Fang)

Received October 26, 2023; Revised December 22, 2023; Accepted December 29, 2023

ABSTRACT

- Agricultural activities may promote the conversion of inorganic Hg to MeHg in soil.
- Hg and As present an extremely and a moderately contaminated level, respectively.
- The human health risks posed by As, Hg, and Ni merit more attention.
- Pokeweed may be considered as a potential Hg hyperaccumulator.

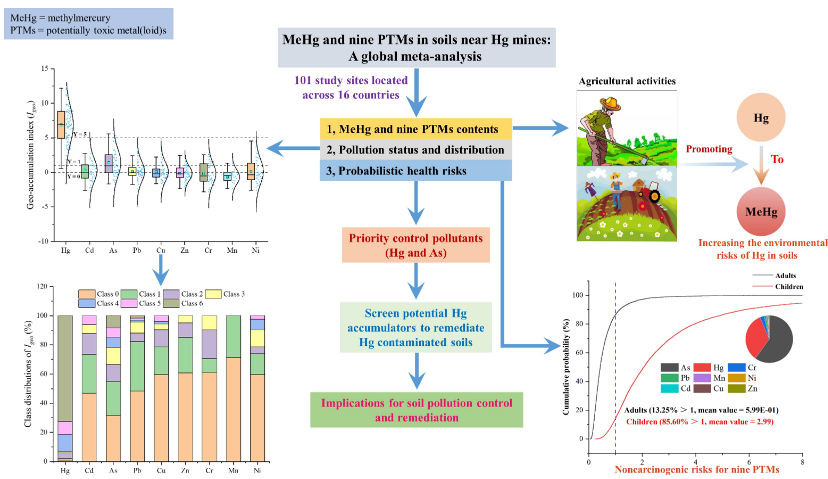

Soil pollution caused by potentially toxic metal(loid)s (PTMs) near mercury (Hg) mines has attracted extensive attention, yet the status and potential health risks of PTM contamination in soils near Hg mining sites have rarely been investigated on a large scale. Global data on methylmercury (MeHg), Hg, Cd, Cr, As, Pb, Cu, Zn, Mn, and Ni concentrations in soils from Hg mining areas were obtained from published research articles (1999–2023). Based on the database, pollution levels, spatial distributions, and potential health risks were investigated. Results indicated that the average percentage of MeHg to total Hg in agricultural soils (0.19%) was significantly higher than that in non-agricultural soils (0.013%). Indeed, 72.4% of these study sites were extremely contaminated with Hg. Approximately 45% of the examined sites displayed a moderate level of As contamination or even more. Meanwhile, the examined sites in Spain and Turkey exhibited considerably higher pollution levels of Hg and As than other regions. The mean hazard indices of the nine PTMs were 2.91 and 0.59 for children and adults, with 85.6% and 13.3% of non-carcinogenic risks for children and adults that exceeded the safe level of 1, respectively. In addition, 70.2% and 56.7% of the total cancer risks through exposure to five carcinogenic PTMs in children and adults, respectively, exceeded the safety level. As and Hg showed a high exceedance of non-carcinogenic risks, while As and Ni were the leading contributors to carcinogenic risks. This study demonstrates the urgent necessity for controlling PTM pollution and reducing the health risks in soils near Hg mining sites and provides an important basis for soil remediation.

Keywords Hg mines, potentially toxic metal(loid)s, soil pollution, probabilistic health risks, remediation strategies, A global meta-analysis

1 Introduction

Mercury (Hg) is a global contaminant owing to its long-distance transportation and persistence in the environment (Li et al., 2012; O'Connor et al., 2019). Hg can exist in gaseous elemental form (Hg^0) that is very stable, with a residence time of several months to over a year (Weiss-Penzias et al., 2016; Saiz-Lopez et al., 2018). Its transport and

Cite this: Soil Ecol. Lett., 2024, 6(4): 240233

deposition pose a significant threat to the global ecosystem because deposited Hg is more readily transformed to methylmercury (MeHg), the most toxic Hg form, under anoxic conditions (Meng et al., 2011; Xu et al., 2017; Man et al., 2021). Mercury mining is considered as one of the most important sources of Hg contamination in the soil environment. Thus far, the demand for Hg products has increased steadily because they are widely used in various industrial activities such as the manufacture of polyvinyl chloride plastic and non-ferrous metal smelting (Ren et al., 2014; Song et al., 2021; Cao et al., 2022). This increased demand further intensifies Hg mining activities. Moreover, large amounts of other potentially toxic metal(loid)s (PTMs) are also released into the soil environment due to destructive Hg mining (González-Fernández et al., 2018; Kulikova et al., 2019; Boente et al., 2022; Barago et al., 2023). These PTMs, including As, Cr, Pb, Cd, Mn, and Ni, are significantly elevated in Hg mining areas (Kulikova et al., 2019; Wu et al., 2020; Liu et al., 2022; Barago et al., 2023). Elevated PTM levels in soils may pose a substantial threat to agricultural production and human health because of their bioaccumulation and toxicity (Tian et al., 2022; Zeng et al., 2022; Chen et al., 2023). Thus, it is urgently needed to evaluate the pollution status of PTMs in soils around Hg mines and analyze their potential human health risks for sustainable mining development.

Soil, an important environmental medium, is a potential medium by which humans are exposed to contaminants (Bing et al., 2021). Toxic metal(loid)s released from Hg mining activities can easily enter agricultural soils and are subsequently transferred to crop plants, which induced a serious threat to sustainable agriculture and human health (Chen et al., 2019; Eagles-Smith et al., 2020). Mercury is one of the most toxic elements that affect endothelial and cardiovascular functions, even at low doses (Natasha et al., 2020; Salmi and Boulila, 2021). Furthermore, Hg toxicity includes kidney damage, respiratory disorders, and disruption of the nervous system (Li et al., 2022). Similarly, As exposure can also result in liver and kidney damage in humans and even induce cancer (Zeng et al., 2019; Wei et al., 2019). Indeed, the exposure pathway of soil PTMs mainly includes dermal absorption, ingestion, and inhalation. Compared to adults, children are more susceptible to soil PTMs due to their special behavior and weak resistance (Peng et al., 2022; Wu et al., 2023). The PTM input in soils from Hg mining areas has increased continuously in the last few decades, which may elevate human health risks from exposure to PTMs (Crespo-Lopez et al., 2021; Zhang et al., 2023). Insufficiently, nearly all studies regarding soil PTM contamination near Hg mining sites associated with human health risk assessment have been conducted in limiting area, while less research has been conducted at a national/global level. In recent years, most researchers investigated the risk assessment of exposure to PTM-contaminated sites based on the total concentrations of PTM and related exposure parameters (Ran et al., 2021; Yuan et al., 2021). However, this may cause a fuzzy estimation on the health risk because of the spatial heterogeneity of PTMs in soils and complex environmental conditions (Guan et al., 2022). Monte Carlo simulation is a widely used random sampling method recommended by the USEPA and National Academy of Sciences, which properly considers variable factors in a complex environment (Yang et al., 2020; Guan et al., 2022). Monte Carlo simulation can effectively decrease uncertainty in various exposure parameters such as total PTM concentrations, intake rate, and toxicity criteria (Liu et al., 2021a; Guan et al., 2022). A recent study assessed potential health risks of PTMs in agricultural soils across China by coupling meta-analysis and Monte Carlo simulation (Guo et al., 2023). Similarly, Wei et al. (2023) demonstrated PTM concentrations in rice that meet safety standards could still pose potential health risk to human based on a national meta-analysis associated with Monte Carlo simulation. This provides a scientific basis for reducing the potential human health risk and proposing the efficient remediation strategies.

Phytoremediation has been successfully applied to remediate Hg contaminated soils in practice due to its sustainable, low-cost, and environmentally-friendly method as compared to traditional physical or chemical strategies (Raj et al., 2020; Liu et al., 2021a; Baragaño et al., 2022). Shoot bioaccumulation and translocation of Hg are the core of phytoremediation, which depends on the plant species (Fernández et al., 2017). Thus far, a few plant species have been shown to hyper-accumulate Hg in their aerial parts (Chamba et al., 2017; Liu et al., 2021a). Thus, more studies are required to screen for potential Hg hyperaccumulators. Indeed, native plant species growing in Hg mining areas are considered potential candidates for remediating Hg-contaminated sites. This is because they can adapt to the chemical stress derived from exposure to Hg and the particular ambient climatic conditions of the contaminated sites (Chamba et al., 2017; Antoniadis et al., 2021). Furthermore, exotic plant species pose potential ecological risks to local ecosystems (Antoniadis et al., 2021). Therefore, a comprehensive study of the ability of native plant species to take up Hg in heavily contaminated areas is valuable for remediating contamination and reducing human exposure risk.

A comprehensive meta-analysis of MeHg and nine PTMs (Hg, Cd, Cr, As, Pb, Zn, Cu, Mn, and Ni) contents in Hg mine-associated soils at the global scale was conducted based on published and peer-reviewed original articles from 1999 to 2023. We hypothesize that these soil PTMs in soils may result in serious contamination and pose potential risks to human health. Our main aims were to 1) evaluate the levels of PTM contamination in Hg mine-associated soils;

2) investigate the spatial distributions of soil PTMs pollution from Hg mining sites worldwide; 3) assess the probabilistic health risks of soil PTMs to human; and 4) analyze the potential of plant species for the remediation of Hg-polluted soils.

2 Study methods and data source

2.1 Literature synthesis and data collection

A database of MeHg and PTM concentrations in soils near Hg mining sites was compiled based on the original papers published between 1999 and 2023 (Tables S1−S3). The key search terms such as “metal,” “metalloid” or “individual PTM (i.e., Hg, Cd, As, Pb, Cu, Cr, Zn, Mn, and Ni)” with “soil” and “mercury mine” were used on ISI Web of Science, Science Direct, Google Scholar, and China National Knowledge Infrastructure to search relevant literature. Finally, data from 100 research papers focused on the concentrations of MeHg and nine priority PTMs in soil from Hg mining areas were extracted by WebPlotDigitizer software. The literature selected for our meta-analysis met the following criteria (Fig. S1): 1) samples were collected from surface soils in Hg mining areas via random sampling methods and sediment samples were eliminated; 2) the number of soil sampling sites, coordinates of the Hg mining area, and background values of PTM were obtained; 3) these samples were mixed, dried, crushed, and sieved until powders were obtained for subsequent use; and 4) MeHg and PTM contents in the soil samples were analyzed using acceptable methods and analytical tools. The sampling information, analytical methods, and quality control in the literature are listed in Table S1.

In this meta-analysis, land use types were differentiated into two subgroups, including 31 agricultural sites and 70 non-agricultural sites from Hg mining areas worldwide. Furthermore, Hg concentrations in 172 native plant species grown in mining areas were obtained from 13 research papers as a new data set (Table S4). Hg concentrations in 55 plant species grown in Hg-polluted soils under pot conditions were collected from 29 academic articles (Table S5). Shoot Hg and Hg concentrations in rhizosphere soils were obtained from the collected literature.

2.2 Soil pollution and ecological risk assessment

Geo-accumulation (I_{geo}) is one of the most widely-used pollution indices because of its accuracy. It is performed by calculating Eq. (1) (Liu et al., 2021b; Ramazanova et al., 2021):

$$I_{geo} = \log_2\left(\frac{C_i}{1.5B_i}\right) \tag{1}$$

where C_i is the measured concentration of each PTM i in the soil (mg kg^{-1}); B_i represents the background value of toxic metal(loid) i in the soil in the study area. A seven-category ranking system (classes 0 to 6) was applied to differentiate the pollution levels, which was provided in Table S6 (Liu et al., 2021b). The potential ecological risks of PTMs in Hg mine-associated soils is assessed using Potential Ecological Risk Index (*PERI*) Method (Eqs. (2)–(4): Pobi et al., 2020; Yang et al., 2022)

$$CF_i = \frac{C_i}{B_i} \tag{2}$$

$$E_r{}^i = T_r{}^i \times CF_i \tag{3}$$

$$PERI = \sum E_i \tag{4}$$

where CF_i is the ratio of PTM i concentration in the soil to background value of PTM in soils; E_r^i is the potential ecological risk of a single PTM I; T_r^i represents the toxic response factor for toxic metal(loid) i, and T_r^i of Hg, Cd, As, Pb, Cu, Zn, Cr, Mn, and Ni is 40, 30, 10, 5, 5, 1, 2, 5, and 5, respectively (Ma et al., 2020; Pobi et al., 2020). The potential ecological risks of soil PTMs from Hg mining areas were divided into five classes, as provided in Table S7 (Yang et al., 2022).

2.3 Health risk assessment models

2.3.1 Exposure risk assessment

Health risk assessment models proposed by the United States Environmental Protection Agency can effectively quantify carcinogenic and non-carcinogenic effects of perpetual exposure to PTMs on human health (Yang et al., 2020). The health risks arising from soil PTMs in Hg mining areas were assessed by considering three exposure routes (1) oral ingestion, (2) inhalation, and (3) dermal absorption. The non-carcinogenic risk from soil PTMs is calculated by the hazard quotient (*HQ*) by estimating the average daily intake (*ADI*, mg kg^{-1} d^{-1}) of each PTM. The *ADI* of the PTM via these routes was calculated using Eqs. (5) to (8):

$$ADI_{ing} = \frac{c \times IngR \times CF \times EF \times ED}{BW \times AT_{\frac{nc}{ca}}} \tag{5}$$

$$ADI_{inh} = \frac{c \times InhR \times EF \times ED}{PEF \times BW \times AT_{\frac{nc}{na}}} \tag{6}$$

$$ADI_{derm} = \frac{c \times SA \times SL \times ABS \times EF \times ED}{BW \times AT_{\frac{nc}{ca}}} \times 10^{-6} \tag{7}$$

$$ADI_{total} = ADI_{ing} + ADI_{inh} + ADI_{derm} \tag{8}$$

where ADI_{ing}, ADI_{inh}, and ADI_{derm} represent ingestion, inhalation, and dermal routes of *ADI*, respectively. All detailed information is presented in Table S8.

2.3.2 Non-carcinogenic risk assessment

For non-carcinogenic risk, the hazard quotient (*HQ*) was used to estimate carcinogenic risks from each exposure route (Eq. (9)), and the carcinogenic risks of all exposure routes was calculated using the hazard index (*HI*, Eq. (10)) (Liu et al., 2021b):

$$HQ = \frac{ADI_{total}}{RfD} \tag{9}$$

$$HI = \sum HQ = HQ_{oral} + HQ_{dermal} + HQ_{inh} \tag{10}$$

where *RfD* indicates the reference dose (mg kg^{-1} d^{-1}; Table S7). *HQ/HI* values < the safe level of 1 represents no adverse effects in humans; otherwise, *HQ/HI* value high than 1 suggests non-carcinogenic risks (Yang et al., 2020).

2.3.3 Carcinogenic risk assessment

The carcinogenic risk (*CR*) of individual carcinogenic PTMs (Cd, Cr, Ni, As, and Cu) in soils across all exposure routes was calculated using Eq. (11), whereas the total carcinogenic risks (*TCR*s) was computed using Eq. (12):

$$CR = ADI \times SF \tag{11}$$

$$TCR = \sum CR = CR_{\text{oral}} + CR_{dermal} + CR_{inh} \tag{12}$$

where *SF* is carcinogenicity slope factor (mg kg^{-1} d^{-1}, Table S9); A *TCR* value below 1×10^{-4} indicates a safe or negligible level, but *TCR* exceeding this threshold suggests a non-negligible cancer risk (Guan et al., 2022).

2.4 Monte Carlo simulation

Monte Carlo simulation has been widely applied to analyze the distribution of human health risks by properly considering variable factors in a complex environment (Khodadadi et al., 2022; Guan et al., 2022; Zhao et al., 2022). To reduce heterogeneity of variations in risk analysis, it was employed to handle uncertainty in soil PTM concentrations, body-weight, exposure frequency, toxicity criteria, and various exposure parameters (Liu et al., 2021b). In this meta-analysis, the Monte Carlo simulation was run for 10000 iterations using Oracle Crystal Ball software (11.1.2.3.000) to achieve reliable results for human health risks. In addition, all detailed information is presented in Table S10.

2.5 Data analysis

Statistical analysis of all data was conducted in Microsoft Excel 2021. All figures were generated using OriginPro 9.2. The worldwide spatial variations in soil PTM pollution from the Hg mining area were determined using ArcGIS 10.2. The cumulative probabilities of human health risk were evaluated using Monte Carlo simulation which was performed using the Oracle Crystal Ball software (11.1.2.3.000). SPSS 25 was used to assess significant differences between the agricultural soils and non-agricultural soils via a Mann–Whitney U test.

3 Results and discussion

3.1 Concentrations of MeHg and nine PTMs in the soils

The concentrations of MeHg and nine PTMs were obtained from over 10000 soil samples from Hg mining areas across 16 countries. Descriptive statistics for the contaminant concentrations are summarized in Table 1. The average concentration of Hg (135 mg kg^{-1}) in the soils was greater than two thousand times the global background value (Table 1), suggesting that Hg-rich contaminants are released into the soil environment during mining activities. Moreover, Hg readily accumulated in the topsoils (0–20 cm). Hg concentrations decreased by more than 80% at 80–100 cm soil depths (Fig. 1). Previous studies have indicated that the concentration of labile Hg, including water-soluble,

Table 1 The statistic analysis of MeHg (μg kg^{-1}) and PTMs (mg kg^{-1}) in soils near Hg mining sites.

MeHg and PTMs	10th	90th	Median	Average	Standard deviation	Coefficient of variation	Sample No.	Global average (mg kg^{-1})
MeHg	1.64	21.6	3.66	7.97	10.6	133%	404	-
Hg	2.67	261	41.8	135	336	249%	14556	0.07
Cd	0.20	2.41	0.83	1.78	4.30	241%	11937	0.41
As	9.29	430	34.8	129	237	184%	12251	6.83
Pb	16.7	171	49.0	86.3	131	152%	13268	27
Cu	21.1	167	41.6	103	214	208%	3924	38.9
Zn	58.1	326	107	150	122	81.4%	13103	64
Cr	20.5	385	69.0	156	213	136%	11409	59.5
Mn	318	1562	685	846	590	69.7%	1486	571
Ni	17.2	461	36.4	190	404	213%	2725	29.0

exchangeable, and carbonate forms of Hg complexes, in soils from Hg mining areas is extremely low, resulting in low mobility (Fernández-Martínez et al., 2019; Quintanilla-Villanueva et al., 2020). The average MeHg concentrations and their average percentages of total Hg concentrations were 7.97 μg kg^{-1} and 0.74%, respectively (Fig. 2). The percentages of most study sites were similar below 0.05%. However, the percentage (0.94%) of the Itomuka Hg mining area was significantly higher than that of other Hg mining areas (Kodamatani et al., 2022) (Fig. 1). The soil organic matter (SOM) content and its decomposition are key factors in the formation of MeHg, while Hg methylation by microbes occurs preferentially under reducing conditions (Tomiyasu et al., 2012; Fernández-Martínez et al., 2015; Kodamatani et al., 2022). Forest soils near the Itomuka Hg mine have high levels of SOM and a relatively high decomposition rate of SOM, resulting in the strong Hg methylation ability of these soils (Kodamatani et al., 2022). The average percentage of MeHg was significantly higher in the agricultural lands (0.19%) than in the non-agricultural lands (0.013%), which is also solid evidence for our above-mentioned explanation (Fig. S2). This might be attributed to agricultural soils with high microbial activities providing favorable conditions for the decomposition of SOM (Fernández-Martínez et al., 2015; Kodamatani et al., 2022). Therefore, it is worth noting that agricultural activities may induce a high environmental risk in Hg mining areas.

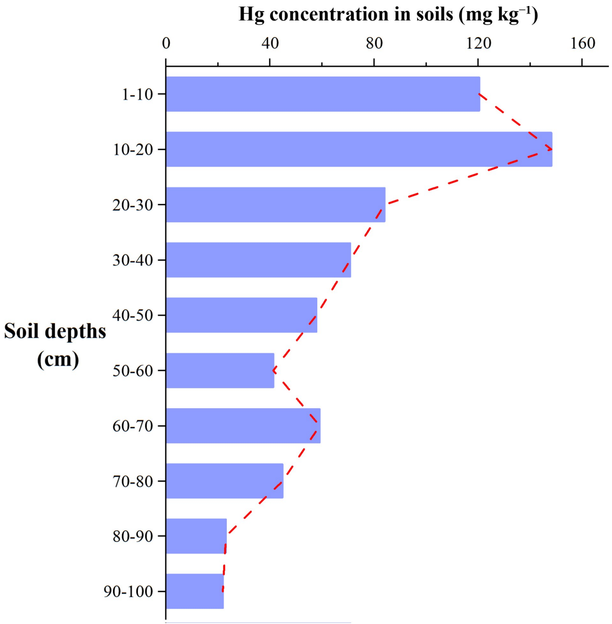

Fig. 1 Soil depth profiles of Hg concentrations in soils from Hg mining areas. Data were from five independent studies (Qiu et al., 2006; Sun et al., 2009; Hojdová et al., 2009; Li et al., 2012; Li, 2013). Note: seven sampling sites on the soil depth profiles of Hg concentrations were obtained from five independent studies. The red dashed line represents trend of Hg migration in various soil depth profiles.

The mean concentrations of Cd, As, Pb, Cu, Zn, Cr, Mn, and Ni in the soil were 1.78, 129, 86.3, 103, 150, 156, 846, and 190 mg kg^{-1}, respectively, which were higher than the average global soil values (Table 1). The mean concentrations of Cd, As, and Ni were 4.34, 18.9, and 6.55 times than their average global soil values, respectively. These results suggest that Hg mining activities increase the accumulation of PTMs in surface soils, thereby inducing high environmental risk. A possible reason for this result is that realgar (AsS) and orpiment (As_2S_3) are important minerals associated with Hg mining processes (Ordóñez et al., 2011; Silva et al., 2014). Moreover, soil Ni and Cd enrichment in Hg mining areas may be related to the lithological composition of the bedrock (Podolský et al., 2015; Kulikova et al., 2019; Hiller

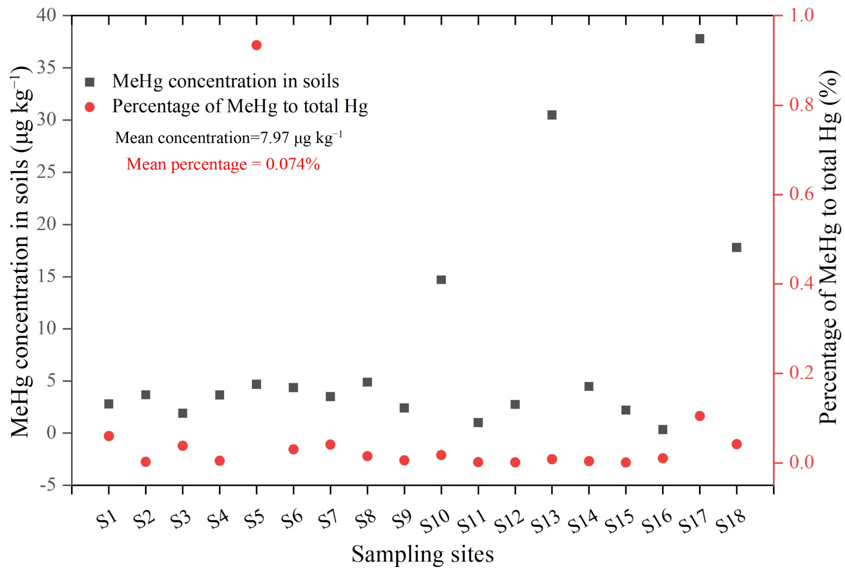

Fig. 2 MeHg concentrations (μg kg^{-1}) and their percentage (%) of total Hg in soils near Hg mines. Note: S1–S18 represent soils near 18 Hg mining sites worldwide from 18 independent studies. (Detailed information is provided in Table S3)

et al., 2021). Indeed, conglomerates with pebbles of ultrabasic rocks in Hg mining areas are enriched in high levels of Ni (Kulikova et al., 2019; Hiller et al., 2021).

The coefficient of variation (CV) is an important indicator that quantifies the average variation in soil PTM concentration (Xie et al., 2022). In this meta-analysis, the CV values of different PTM concentrations are the decreasing order of Hg > Cd > Ni > Cu > As > Pb > Cr > Zn > Mn (Table 1). This result suggests a remarkable variation in PTM concentrations in soils. There are several possible explanations for this phenomenon. First, wind direction and intensity play crucial roles in influencing the PTM transportation process, especially for gaseous Hg (Ballabio et al., 2021). Meanwhile, atmospheric deposition is an important resource for soil Hg pollution, which is easily controlled by various factors (Chen et al., 2022). Second, temperature and precipitation pose indirect influences on the distribution of PTM concentrations in soils near Hg mining sites (Yuan et al., 2021). Moreover, PTM accumulation in topsoils is also influenced by other factors, such as land-use type, geologic setting, and exploitation method (Li et al., 2012; Hiller et al., 2021; Peng et al., 2022).

3.2 Contamination assessment of PTMs in the soils

The I_{geo} values of the nine PTMs in the soils and their percentage distributions are illustrated in Fig. 3. The mean I_{geo} of Hg, Cd, As, Pb, Cu, Zn, Cr, Mn, and Ni were 6.73, 0.17, 1.34, 0.20, 0.16, −0.13, −0.17, −0.61, 0.14, respectively (Fig. 3A). According to the distribution of the I_{geo} values, more than 60% of these study sites for these PTMs (i.e. Cu, Zn, Cr, Mn, and Ni) were situated in class 0 (Fig. 3B), suggesting that most of Hg mining areas were uncontaminated by the five PTMs. For Cd and Pb, more than 70% of the I_{geo} values were below class 2. The mean I_{geo} of As was in class 2, while ~45% of the As sampling sites were above class 2 (Fig. 3A and 3B). This result indicates that As showed a moderate contamination level in soils near the Hg mines. For most Hg mining areas, cinnabar (HgS) is the main mineral phase, while it is disseminated through the host rock or is located in realgar (AsS) and orpiment (As_2S_3) (Ordóñez et al., 2011). We also observed that the ecological risks from Cd and As are nonnegligible in Hg mining areas (Table S11). In addition, the I_{geo} of Hg in 72.4% of the examined sites were situated in class 6, and Hg pollution causes an extremely high ecological risk in this area (Fig. 3B). These findings demonstrated that most of the study sites were extremely contaminated by Hg and it has caused high environmental risks. Kulikova et al. (2019) reported that mine waste heaps contain high levels of Hg, which are the predominant source of soil Hg pollution. Moreover, roasting of Hg ores is considered an important source of Hg in the soil environment because of the emission of gaseous Hg compounds (Higueras et al., 2013; Kulikova et al., 2019). However, it is difficult to quantify its contribution to overall Hg pollution in Hg mining areas.

The PTM pollution levels in the soils were influenced by land use, as shown in Fig. 4. In this study, the pollution levels of all PTMs in non-agricultural lands were higher than those in agricultural lands. Indeed, the accumulation of PTMs in surface soils is easily influenced by the distances between the study sites and centers of Hg mines. Agricultural activities are generally carried out farther from the centers of Hg mines (Liu et al., 2022). These five PTMs (Pb, Cu, Zn, Cr, and Ni) exhibited uncontaminated to moderate pollution in non-agricultural soils, but the agricultural soils were practically uncontaminated by these PTMs (Fig. 4). As mentioned above, agricultural soils are located in areas distant from Hg mining sites. Therefore, this phenomenon also indirectly supports the view that PTMs enriched in non-agricultural soils near Hg mining sites may be geogenic (Kulikova et al., 2019; Horasan, 2020; Hiller et al., 2021).

3.3 Pollution distributions of PTMs

The pollution distribution of PTMs in Hg mining areas is

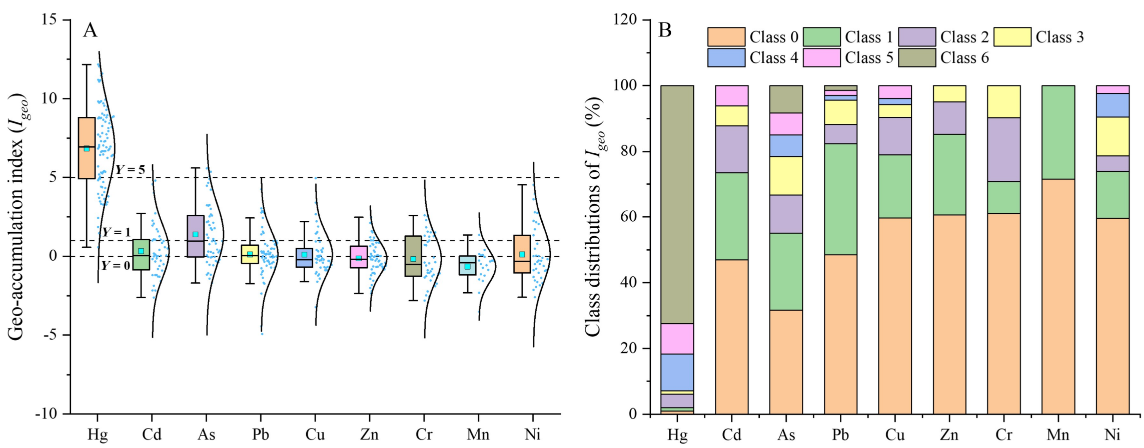

Fig. 3 Geo-accumulation indices of nine PTMs (A) and their percentage distributions (B) in Hg mine-associated soils.

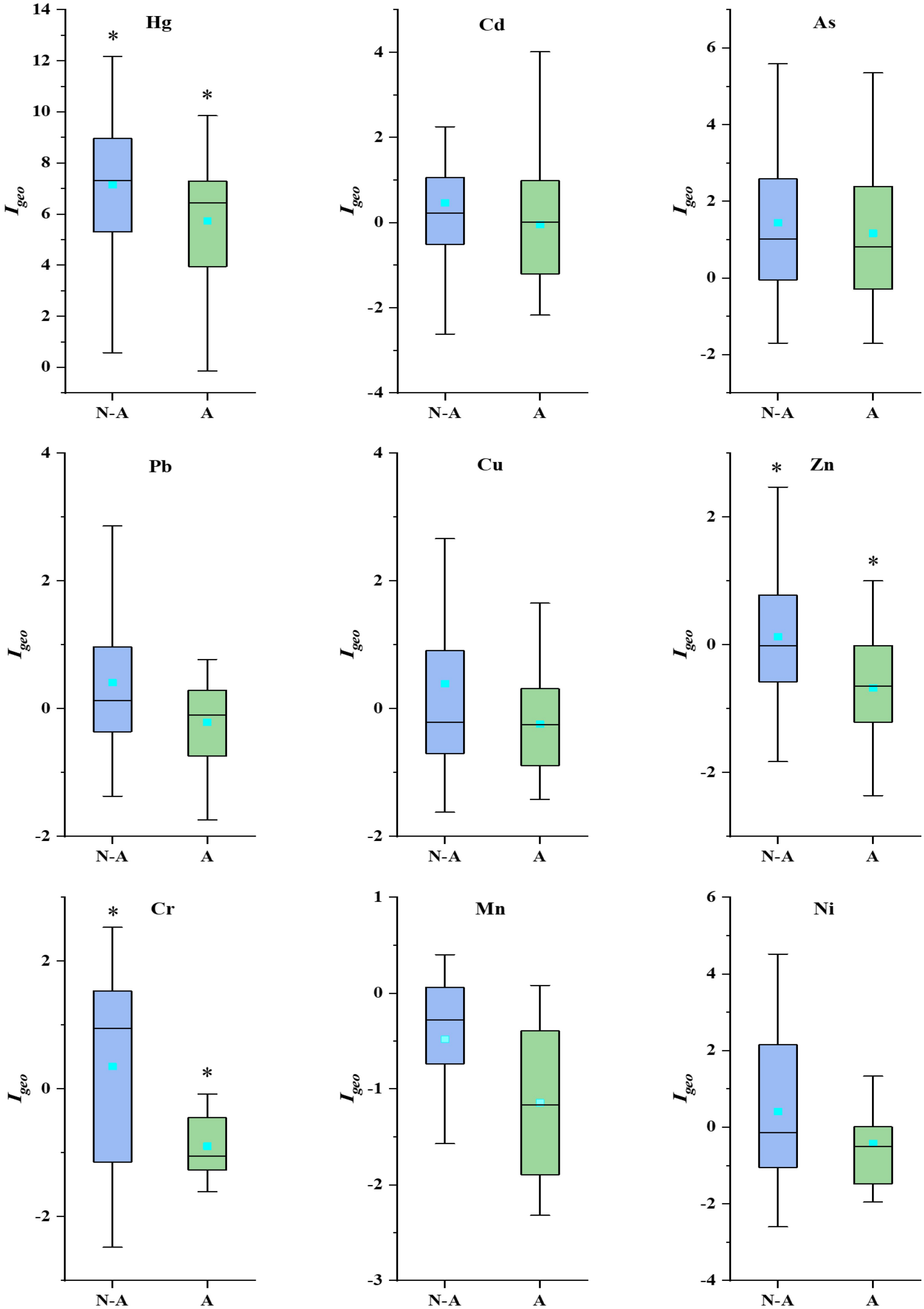

Fig. 4 Geo-accumulation indices of nine PTMs in agricultural soils (A) and non-agricultural soils (N–A) from Hg mining areas. Note: "*" represents the significant differences between agricultural soils and non-agricultural soils via a Mann–Whitney U test.

presented in Table S12. Most of the examined sites were located in China, Spain, Slovenia, and Turkey. Their average I_{geo} values for Hg were 6.53, 5.53, 7.33, and 7.25, respectively (Table S12). The Hg pollution levels in most study sites were situated in class 6, revealing that Hg pollution in soils near Hg mines is extremely serious worldwide. In addition, the sites examined in Spain, Turkey, and Namibia were heavily contaminated by As. In our meta-analysis, the highest pollution level in soils from Hg mining areas was observed in Zambia for Cu (4.95), Spain for Mn (1.35), the Philippines for Ni (3.94), Namibia for Pb (4.25) and Zn (2.47), and China for Cd (4.56) and Cr (2.59) (Fig. 5). The difference in these seven PTM pollutants from Hg mining areas may be related to geogenic factors rather than anthropogenic factors (Horasan, 2020; Hiller et al., 2021). However, the specific mechanisms remain unknown.

3.4 Health risk assessment of PTMs in the soils

3.4.1 Non-carcinogenic risks of PTMs

In the meta-analysis, the ingestion route contributed to 56.3% and 69.7% of the non-carcinogenic risk for adults and children, respectively (Fig. 5A). The mean *HQ* values displayed a decreasing trend of $HQ_{ing} > HQ_{dermal} > HQ_{inh}$. This indicated that ingestion is an important route of exposure to PTMs in soils from Hg mining areas. This finding is agreement with those reported by Tang et al. (2021) and Xu et al. (2020). The *HI* values of PTMs for local children were significantly higher than those for local adults, suggesting that the soil PTM pollution may induce a higher health risk to children (Fig. 5B). A similar result was reported by Guan et al. (2022), showing that children are more susceptible to PTMs in urban agriculture soils of a typical oasis city as compared to adults. This result is due to the peculiar physiology and behavior of children, including a high respiration rate and finger sucking (Liu et al., 2021b; Guan et al., 2022).

The mean *HI* values were 2.91 for children and 0.59 for adults, respectively (Fig. 5). Despite that the mean *HI* values of adults were far below the safety threshold of 1, this does not imply that these PTMs do not pose health risks to adults living in Hg mining areas. In some of the examined sites, the health risks to adults exposed to PTMs in the soils exceeded the safety level. As shown in Table S13 and Fig. 5B, the mean *HI* values for the individual PTM increased in the order Zn < Cu < Cd < Ni < Mn < Pb < Cr < Hg < As. The *HI* values of As and Hg for children were 60 and 33.58% of the *HI* values of all PTMs, respectively (Fig. S4). Furthermore, the children's *HI* value was 1.60 and 1.09 for As and Hg, respectively, exceeding the safety threshold of 1.0. This finding revealed the health risks of As and Hg in soils to children. Therefore, As compounds can pose strong effects on a variety of human organisms, including the skin, intestine, stomach, weasand, and brain (Bali and Sidhu, 2021; Rehman et al., 2021). Meanwhile, Hg is also highly toxic to human health and can induce multiple adverse reactions,

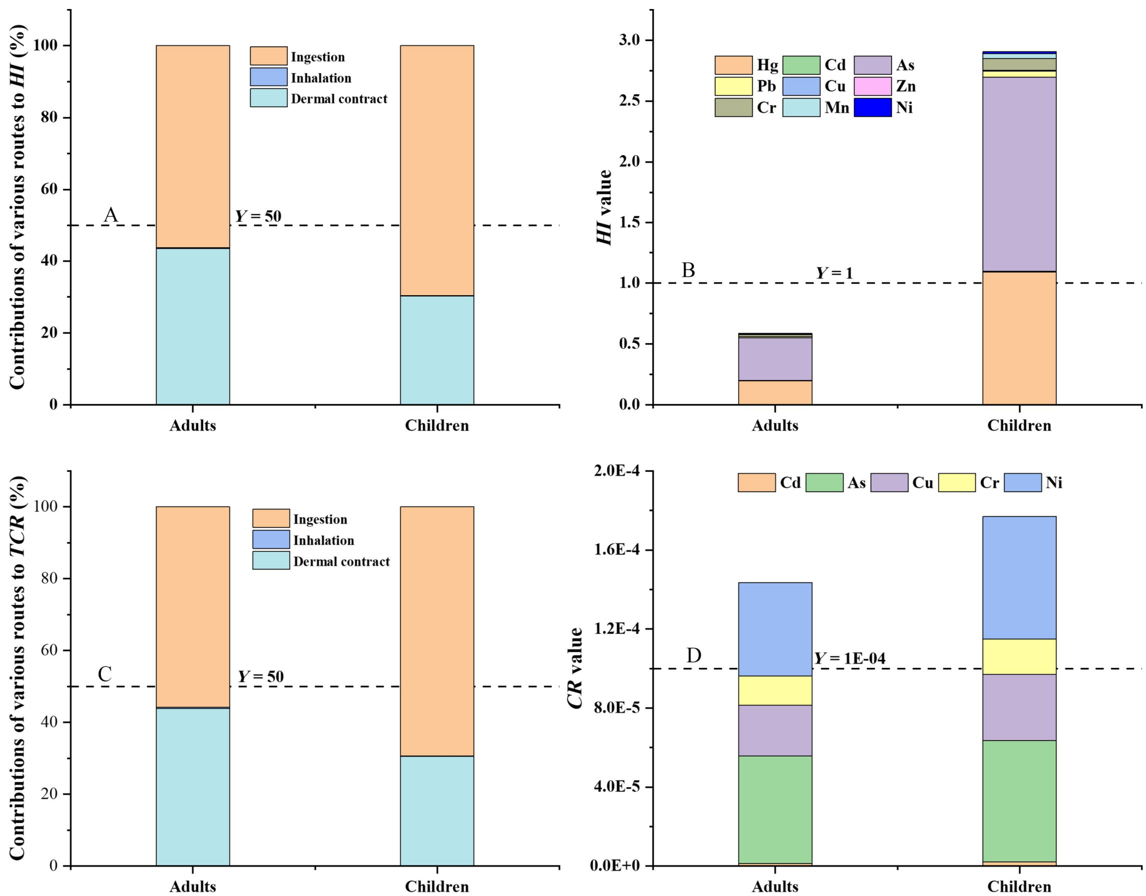

Fig. 5 Contributions of three exposure routes (ingestion, inhalation, and dermal contact) to non-cancer (A) and cancer risks (C), and hazard index (B) and cancer risk (D) of the nine PTMs in the soils.

including stomach ache, diarrhea, renal failure, and gastrointestinal perforation (Huang et al., 2022; Feng et al., 2022). In addition, other PTMs in soils, such as Cd, Zn, Cu, and Ni, induced no non-cancer risk to local inhabitants due to their low contribution rates to total *HI* values (< 1%) (Fig. S3).

3.4.2 Carcinogenic risk of PTMs

Similar to the above-mentioned results, the *CR* for ingestion was higher than that for both inhalation and dermal contraction (Fig. 5C). Meanwhile, the total *CR* values of children for each PTM were markedly lower than those of adults, which provided direct evidence that children were more susceptible to PTMs (Fig. 5D). In this meta-analysis, the total *CR* values of these PTMs for adults and children were 1.44E–04 and 1.77E–04, respectively, revealing the presence of carcinogenic risks for human living in Hg mining areas, because their total *CR* values in the soils exceeded the safety threshold of 1E–04. In addition, the contribution rates of As and Ni were 70.92 and 69.92% for adults and children (Fig. S4), respectively. These results suggest that As and Ni are the primary carcinogenic PTMs in soils.

3.5 Risk characterization based on Monte Carlo simulation

The health risk results of the nine PTMs in soils around Hg mining sites based on Monte Carlo simulations are shown in Fig. 6. As mentioned above, although the mean *HI* value for local adults was below the safe threshold of 1, 13.3% of their *HI* distribution exceeded the safe level (Fig. 6A). Moreover, the average *HI* value for children was substantially higher than the toxic effect value, with 85.6% of the children's *HI* values > 1 (Fig. 6A). Among these PTMs, the contribution of As to children's non-carcinogenic risks was the highest, followed by Hg and Cr (Fig. S3). Meanwhile, 29.6% and 42.2% of the children's *HI* values for Hg and As were > 1, respectively. However, none of the *HI* values of Cd, Cu, Ni, Zn, and Mn for adults and children exceeded 1 (Fig. S5).

As shown in Fig. 6B, the *TCR* for local children and adults were 70.2% and 56.7%, respectively, higher than the carcinogenic risk threshold (1E–04). These results indicate that children have a higher percentage of *TCR* values exceeding the safe level than adults. Among the carcinogenic PTMs, As and Ni were the primary contributors to *TCR* values, accounting for 37.9% (34.8%) and 33.2% (35.1%) for adults (children), respectively (Fig. S4). Meanwhile, 13.7% and 11.8% of the As *CR* values for local children and adults, respectively, were greater than the safe level (Fig. S6). For Ni, ~16.8% and 11.0% of the *CR* values for local children and adults, respectively, exceeded the threshold value (Fig. S6).

3.6 Remediation of Hg contaminated sites by screening potential Hg accumulator

For soils near Hg mines, Hg and As are the main contaminants derived from mining activities, resulting in serious risks to the ecological system and human health. The environmental risks posed by Cd and Ni in soils cannot be ignored. Overall, Hg should be preferentially controlled compared with As, Cd, and Ni because Hg causes more serious pollution in soils. Remediation techniques for Hg-contaminated soil include soil washing, stabilization, thermal treatment, and phytoremediation (Xu et al., 2015; Wang et al., 2020). Among these techniques, phytoremediation has been widely used to remediate heavily Hg-contaminated soils because of its low cost, ease of use, and eco-friendliness (Singh et al., 2022; Baragaño et al., 2022). The shoot accumulation factor (SAF) of *Cyrtomium macrophyllum* for Hg was the highest (22.3) among 55 plant species growing in

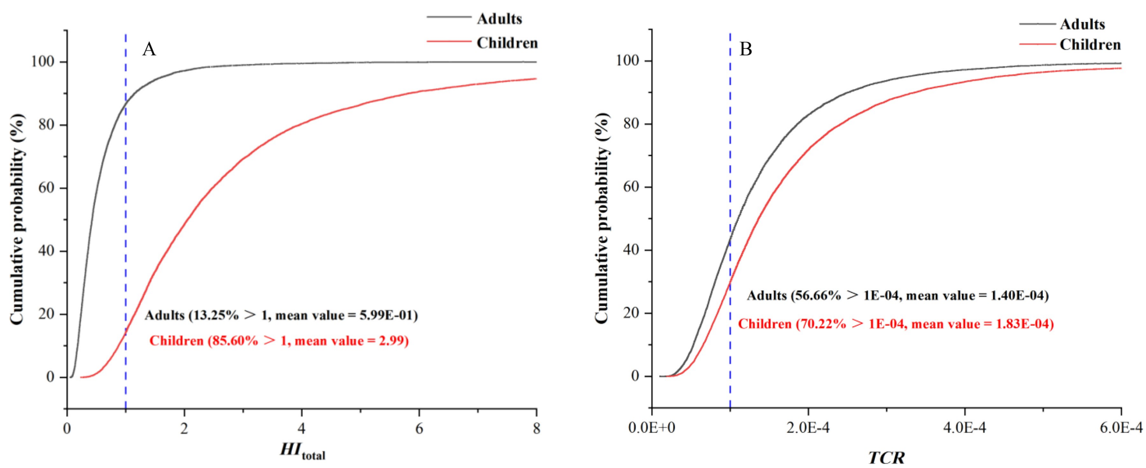

Fig. 6 Probability distribution of the total hazard index (A) and total cancer risk (B). Note: The blue dashed vertical lines represent the safety thresholds of hazard index (A) and cancer risk (B).

Hg-polluted soils under pot conditions (Table S5 and Fig. S7). However, we observed an extremely low SAF (0.012) for *Cyrtomium macrophyllum* grown in the Hg mining area (Table S4). This phenomenon may be due to the additional Hg solution applied to the pot soils, which resulted in a high level of Hg bioavailability (Xun et al., 2017). Indeed, low Hg bioavailability in mining areas has been demonstrated in numerous studies (Lin et al., 2010; Xun et al., 2017; Yin et al., 2018). Thus, screening of potential Hg hyperaccumulators should be prioritised under real field conditions.

In this meta-analysis, the SAF was 1.05 for pokeweed (*Phytolacca americana* L.) and 1.01 for pepper (*Capsicum annuum* L.) (Fig. 7). Among the 172 native species, they exhibited greater potential for remediating Hg-contaminated sites (Table S4). However, pepper is a crop plant with relatively low biomass. Therefore, it is not suitable for phytoremediation. Pokeweed is a perennial herb with high biomass and fast growth rate and is widely distributed globally. In addition, pokeweed shows a strong ability to absorb various PTMs, including Cd, As, and Mn, from contaminated soils (Li et al., 2018; Wang et al., 2021). Therefore, pokeweed could be a potential plant species for remediating contaminated soils in Hg mining areas.

3.7 Limitations

Mercury is a unique PTM, and it is liquid over a wide range of ambient temperatures common (Wang et al., 2020). Thus, the pollution status of Hg mining sites may be dynamic owing to the emission and leaching of Hg from the mine waste calcines (Li et al., 2012). However, most studies only investigated the soil pollution of Hg mining sites at a certain stage. The geological conditions can also influence the soil PTM pollution near Hg mines. Therefore, the collected data from different studies may cause some discrepancies due to variations in temporal disparities and geological conditions. Moreover, the behavior of residents is crucial in health risk assessments, but it is difficult to eliminate the errors caused by the differences in human behavior in different regions. In our meta-analysis, the toxicity parameters for soil PTMs were derived from the USEPA guidelines and international research findings to minimize this error. The wind direction and strength are also important factors influencing the spatial distribution and pollution level of PTMs in soils. However, wind direction and strength associated with environmental impacts are lacking in most studies, which limit the accurate evaluation of health risks of PTMs.

4 Conclusion

Soil PTM pollution and its potential health risk in Hg mining areas at the global scale were assessed. Hg concentrations in native plants were also obtained. The results indicated

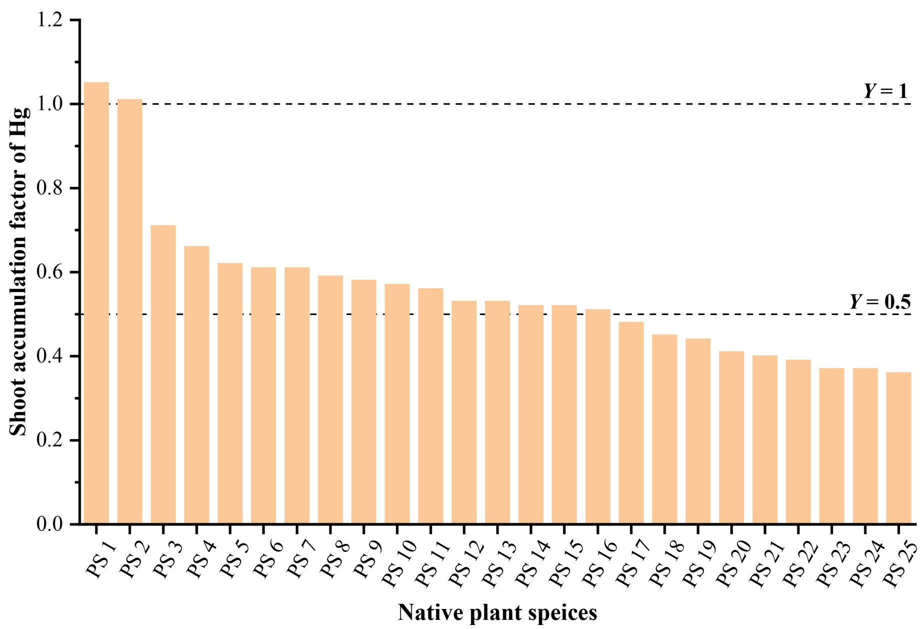

Fig. 7 The top 15% of shoot accumulation factors among the 172 native species were grown in the Hg mining areas. Note: PS 1, *Phytolacca americana* L.; PS 2, *Capsicum annuum*; PS 3, *Chaerophyllum hirsutum* L.; PS 4, *Phyllanthus niruri*; PS 5, *Jatropha curcas*; PS 6, *Senna alata*; PS 7, *Stecherus bifidus*; PS 8, *Potentilla sibbaldii* Haller f.; PS 9, *Tamarix dalmatica* Baum; PS 10, *Plectramthus* sp.; PS 11, *Dittrichia viscosa* (L.) W. Greuter; PS 12, *Eleocharis interstincta*, PS 13, *Piper marginathum*; PS 14, *Guazuma ulmifolia*; PS 15, *Setaria viridis* (L.) Beauv.; PS 16, *Clidemia* sp.; PS 17; *Oxycaryum cúbense*; PS 18, *Pityrogramma colomelanos*; PS 19, *Cyperus luzulae*; PS 20, *Ricinus communis*; PS 21, *Calathea lutea*; PS 22, *Desmodium sequax*; PS 23, *Cinnamomum camphora* (L.) Presl; PS 24, *Rhus chinensis* Mill; PS 25, *Boehmeria pseudotricuspis.*

that agricultural activities may increase the risk of converting Hg to MeHg in soils by enhancing SOM content and its decomposition rate. Hg-rich contaminants were released into the soil environment during mining activities, which led to extreme Hg pollution at most study sites. As is also an important pollutant in soils, resulting in moderate contamination. The pollution levels of Hg and As at the study sites were higher in Spain and Turkey. Furthermore, the ecological risks posed by Cd and As in soil cannot be neglected. Based on the health risk assessments, As and Hg presented high non-carcinogenic risks to residents, whereas As and Ni displayed unacceptable carcinogenic risks. Soil PTMs pollution in Hg mining areas induced a higher risk to children as compared to adults. Therefore, protection measures should be a priority. Therefore, this study revealed the pollution status and health risks posed by exposure to soils from Hg mining areas and presented a viable non-destructive remediation strategy, which provides policymakers with a scientific basis for minimising PTM pollution and reducing health risks.

Declarations of interest

The authors declare that they have not conflict of interest.

Acknowledgments

This work was supported by the Joint Key Funds of the National Natural Science Foundation of China (Grant No. U21A20237), the Strategic Priority Research Program of Chinese Academy of Sciences (Grant No. XDB40020202).

Electronic supplementary material

Supplementary material is available in the online version of this article at https://doi.org/10.1007/s42832-024-0233-7 and is accessible for authorized users.

References

Antoniadis, V., Shaheen, S.M., Stärk, H.J., Wennrich, R., Levizou, E., Merbach, I., Rinklebe, J., 2021. Phytoremediation potential of twelve wild plant species for toxic elements in a contaminated soil. Environment International 146, 106233.

Bali, A.S., Sidhu, G.P.S., 2021. Arsenic acquisition, toxicity and tolerance in plants-From physiology to remediation: A review. Chemosphere 283, 131050.

Ballabio, C., Jiskra, M., Osterwalder, S., Borrelli, P., Montanarella, L., Panagos, P., 2021. A spatial assessment of mercury content in the European Union topsoil. Science of the Total Environment 769, 144755.

Baragaño, D., Forján, R., Álvarez, N., Gallego, J.R., González, A., 2022. Zero valent iron nanoparticles and organic fertilizer assisted phytoremediation in a mining soil: Arsenic and mercury accumulation and effects on the antioxidative system of *Medicago sativa* L. Journal of Hazardous Materials 433, 128748.

Barago, N., Mastroianni, C., Pavoni, E., Floreani, F., Parisi, F., Lenaz, D., Covelli, S., 2023. Environmental impact of potentially toxic elements on soils, sediments, waters, and air nearby an abandoned Hg-rich fahlore mine (Mt. Avanza, Carnic Alps, NE Italy). Environmental Science and Pollution Research 30, 63754–63775.

Bing, H.J., Qiu, S.J., Tian, X., Li, J., Zhu, H., Wu, Y.H., Zhang, G., 2021. Trace metal contamination in soils from mountain regions across China: spatial distribution, sources, and potential drivers. Soil Ecology Letters 3, 189–206.

Boente, C., Baragaño, D., García-González, N., Forján, R., Colina, A., Gallego, J.R., 2022. A holistic methodology to study geochemical and geomorphological control of the distribution of potentially toxic elements in soil. CATENA 208, 105730.

Cao, S.Z., Zhang, L., Zhang, Y., Wang, S.X., Wu, Q.R., 2022. Impacts of removal compensation effect on the mercury emission inventories for nonferrous metal (zinc, lead, and copper) smelting in China. Environmental Science & Technology 56, 2163–2171.

Chamba, I., Rosado, D., Kalinhoff, C., Thangaswamy, S., Sánchez-Rodríguez, A., Gazquez, M.J., 2017. *Erato polymnioides*−A novel Hg hyperaccumulator plant in Ecuadorian rainforest acid soils with potential of microbe-associated phytoremediation. Chemosphere 188, 633–641.

Chen, C.Y., Huang, J.H., Meusburger, K., Li, K., Fu, X.W., Rinklebe, J., Alewell, C., Feng, X.B., 2022. The interplay between atmospheric deposition and soil dynamics of mercury in Swiss and Chinese boreal forests: A comparison study. Environmental Pollution 307, 119483.

Chen, L., Liang, S., Liu, M.D., Yi, Y.J., Mi, Z.F., Zhang, Y.X., Li, Y. M., Qi, J.C., Meng, J., Tang, X., Zhang, H.R., Tong, Y.D., Zhang, W., Wang, X.J., Shu, J., Yang, Z.F., 2019. Trans-provincial health impacts of atmospheric mercury emissions in China. Nature Communications 10, 1484.

Chen, L., Wang, F.Y., Zhang, Z.Q., Chao, H.R., He, H.R., Hu, W.F., Zeng, Y., Duan, C.J., Liu, J., Fang, L.C., 2023. Influences of arbuscular mycorrhizal fungi on crop growth and potentially toxic element accumulation in contaminated soils: A meta-analysis. Critical Reviews in Environmental Science and Technology 53, 1795–1816.

Crespo-Lopez, M.E., Augusto-Oliveira, M., Lopes-Araújo, A., Santos-Sacramento, L., Takeda, P.Y., de Matos Macchi, B., do Nascimento, J.L.M., Maia, C.S.F., Lima, R.R., Arrifano, G.P., 2021. Mercury: What can we learn from the Amazon? Environment International 146, 106223.

Eagles-Smith, C.A., Willacker, J.J., Nelson, S.J., Pritz, C.M.F., Krabbenhoft, D.P., Chen, C.Y., Ackerman, J.T., Grant, E.H.C., Pilliod, D.S., 2020. A national-scale assessment of mercury bioaccumulation in United States national parks using dragonfly larvae as biosentinels through a citizen-science framework. Environmental Science & Technology 54, 8779–8790.

Feng, X.B., Li, P., Fu, X.W., Wang, X., Zhang, H., Lin, C.J., 2022. Mercury pollution in China: implications on the implementation of the Minamata Convention. Environmental Science: Processes & Impacts 24, 634–648.

Fernández, S., Poschenrieder, C., Marcenò, C., Gallego, J.R., Jiménez-Gámez, D., Bueno, A., Afif, E., 2017. Phytoremediation capability of native plant species living on Pb-Zn and Hg-As mining wastes in the Cantabrian range, north of Spain. Journal of Geochemical Exploration 174, 10–20.

Fernández-Martínez, R., Esbrí, J.M., Higueras, P., Rucandio, I., 2019. Comparison of mercury distribution and mobility in soils affected by anthropogenic pollution around chloralkali plants and ancient mining sites. Science of the Total Environment 671, 1066–1076.

González-Fernández, B., Rodríguez-Valdés, E., Boente, C., Menéndez-Casares, E., Fernández-Braña, A., Gallego, J.R., 2018. Long-term ongoing impact of arsenic contamination on the environmental compartments of a former mining-metallurgy area. Science of the Total Environment 610–611, 820–830.

Guan, Q.Y., Liu, Z., Shao, W.Y., Tian, J., Luo, H.P., Ni, F., Shan, Y. X., 2022. Probabilistic risk assessment of heavy metals in urban farmland soils of a typical oasis city in northwest China. Science of the Total Environment 833, 155096.

Guo, G.H., Chen, S.Q., Lei, M., Wang, L.Q., Yang, J., Qiao, P.W., 2023. Spatiotemporal distribution characteristics of potentially toxic elements in agricultural soils across China and associated health risks and driving mechanism. Science of the Total Environment 887, 163897.

Higueras, P., Esbrí, J.M., Oyarzun, R., Llanos, W., Martínez-Coronado, A., Lillo, J., López-Berdonces, M.A., García-Noguero, E.M., 2013. Industrial and natural sources of gaseous elemental mercury in the Almadén district (Spain): An updated report on this issue after the ceasing of mining and metallurgical activities in 2003 and major land reclamation works. Environmental Research 125, 197–208.

Hiller, E., Jurkovič, Ľ., Majzlan, J., Kulikova, T., Faragó, T., 2021. Environmental availability of trace metals (Mercury, Chromium and Nickel) in soils from the abandoned mine area of Merník (Eastern Slovakia). Polish Journal of Environmental Studies 30, 5013–5025.

Hojdová, M., Navrátil, T., Rohovec, J., Penížek, V., Grygar, T., 2009. Mercury distribution and speciation in soils affected by historic mercury mining. Water, Air, and Soil Pollution 200, 89–99.

Horasan, B.Y., 2020. The environmental impact of the abandoned mercury mines on the settlement and agricultural lands; Ladik (Konya, Turkey). Environmental Earth Sciences 79, 237.

Huang, J.L., Wu, Y.Y., Sun, J.X., Li, X., Geng, X.L., Zhao, M.L., Sun, T., Fan, Z.Q., 2021. Health risk assessment of heavy metal(loid) s in park soils of the largest megacity in China by using Monte Carlo simulation coupled with Positive matrix factorization model. Journal of Hazardous Materials 415, 125629.

Huang, Z.L., Yang, Z.B., Xu, X.X., Lei, Y.J., He, J.S., Yang, S., Wong, M.H., Man, Y.B., Cheng, Z., 2022. Health risk assessment of mercury in Nile tilapia (*Oreochromis niloticus*) fed housefly maggots. Science of the Total Environment 852, 158164.

Kan, X.Q., Dong, Y.Q., Feng, L., Zhou, M., Hou, H.B., 2021. Contamination and health risk assessment of heavy metals in China' s lead-zinc mine tailings: a meta-analysis. Chemosphere 267, 128909.

Khodadadi, N., Amini, A., Dehbandi, R., 2022. Contamination, probabilistic health risk assessment and quantitative source apportionment of potentially toxic metals (PTMs) in street dust of a highly developed city in north of Iran. Environmental Research 210, 112962.

Kodamatani, H., Shigetomi, A., Akama, J., Kanzaki, R., Tomiyasu, T., 2022. Distribution, alkylation, and migration of mercury in soil discharged from the Itomuka mercury mine. Science of the Total Environment 815, 152492.

Kulikova, T., Hiller, E., Jurkovič, Ľ., Filová, L., Šottník, P., Lacina, P., 2019. Total mercury, chromium, nickel and other trace chemical element contents in soils at an old cinnabar mine site (Merník, Slovakia): anthropogenic versus natural sources of soil contamination. Environmental Monitoring and Assessment 191, 263.

Li, J.T., Gurajala, H.K., Wu, L.H., van der Ent, A., Qiu, R.L., Baker, A.J.M., Tang, Y.T., Yang, X.E., Shu, W.S., 2018. Hyperaccumulator plants from China: a synthesis of the current state of knowledge. Environmental Science & Technology 52, 11980–11994.

Li, M.L., Kwon, S.Y., Poulin, B.A., Tsui, M.T.K., Motta, L.C., Cho, M., 2022. Internal dynamics and metabolism of mercury in biota: A review of insights from mercury stable isotopes. Environmental Science & Technology 56, 9182–9195.

Li, P., Feng, X.B., Qiu, G.L., Shang, L.H., Wang, S.F., 2012. Mercury pollution in Wuchuan mercury mining area, Guizhou, Southwestern China: The impacts from large scale and artisanal mercury mining. Environment International 42, 59–66.

Li, Y.H., 2013. Environmental contamination and risk assessment of mercury from a historic mercury mine located in southwestern China. Environmental Geochemistry and Health 35, 27–36.

Lin, Y., Larssen, T., Vogt, R.D., Feng, X.B., 2010. Identification of fractions of mercury in water, soil and sediment from a typical Hg mining area in Wanshan, Guizhou province, China. Applied Geochemistry 25, 60–68.

Liu, B.L., Tian, K., He, Y., Hu, W.Y., Huang, B., Zhang, X.H., Zhao, L., Teng, Y., 2022. Dominant roles of torrential floods and atmospheric deposition revealed by quantitative source apportionment of potentially toxic elements in agricultural soils around a historical mercury mine, Southwest China. Ecotoxicology and Environmental Safety 242, 113854.

Liu, H.W., Zhang, Y., Yang, J.S., Wang, H.Y., Li, Y.L., Shi, Y., Li, D. C., Holm, P.E., Ou, Q., Hu, W.Y., 2021a. Quantitative source apportionment, risk assessment and distribution of heavy metals in agricultural soils from southern Shandong Peninsula of China. Science of the Total Environment 767, 144879.

Liu, J., Wang, Y.N., Liu, X.M., Xu, J.M., 2021b. Occurrence and health risks of heavy metals in plastic-shed soils and vegetables across China. Agriculture, Ecosystems & Environment 321, 107632.

Liu, Z.C., Chen, B.N., Wang, L.A., Urbanovich, O., Nagorskaya, L., Li, X., Tang, L., 2020. A review on phytoremediation of mercury contaminated soils. Journal of Hazardous Materials 400, 123138.

Ma, L., Xiao, T.F., Ning, Z.P., Liu, Y.Z., Chen, H.Y., Peng, J.Q., 2020. Pollution and health risk assessment of toxic metal(loid)s in soils under different land use in sulphide mineralized areas. Science of the Total Environment 724, 138176.

Man, Y., Wang, B., Wang, J.X., Slaný, M., Yan, H.Y., Li, P., El-Naggar, A., Shaheen, S.M., Rinklebe, J., Feng, X.B., 2021. Use of biochar to reduce mercury accumulation in *Oryza sativa* L: A trial for sustainable management of historically polluted farmlands. Environment International 153, 106527.

McBride, M.B., Zhou, Y.T., 2019. Cadmium and zinc bioaccumulation by *Phytolacca americana* from hydroponic media and contaminated soils. International Journal of Phytoremediation 21, 1215–1224.

Meng, B., Feng, X.B., Qiu, G.L., Liang, P., Li, P., Chen, C.X., Shang, L.H., 2011. The process of methylmercury accumulation in rice (*Oryza sativa* L.). Environmental Science & Technology 45, 2711–2717.

Natasha, Shahid, M., Khalid, S., Bibi, I., Bundschuh, J., Niazi, N.K., Dumat, C., 2020. A critical review of mercury speciation, bioavailability, toxicity and detoxification in soil-plant environment: Ecotoxicology and health risk assessment. Science of the Total Environment 711, 134749.

O'Connor, D., Hou, D.Y., Ok, Y.S., Mulder, J., Duan, L., Wu, Q.R., Wang, S.X., Tack, F.M.G., Rinklebe, J., 2019. Mercury speciation, transformation, and transportation in soils, atmospheric flux, and implications for risk management: A critical review. Environment International 126, 747–761.

Ordóñez, A., Álvarez, R., Charlesworth, S., De Miguel, E., Loredo, J., 2011. Risk assessment of soils contaminated by mercury mining, Northern Spain. Journal of Environmental Monitoring 13, 128–136.

Pei, P.G., Sun, T., Xu, Y.M., Sun, Y.B., 2021. Soil aggregate-associated mercury (Hg) and organic carbon distribution and microbial community characteristics under typical farmland-use types. Chemosphere 275, 129987.

Peng, J.Y., Zhang, S., Han, Y.Y., Bate, B., Ke, H., Chen, Y.M., 2022. Soil heavy metal pollution of industrial legacies in China and health risk assessment. Science of the Total Environment 816, 151632.

Pobi, K.K., Nayek, S., Gope, M., Rai, A.K., Saha, R., 2020. Sources evaluation, ecological and health risk assessment of potential toxic metals (PTMs) in surface soils of an industrial area, India. Environmental Geochemistry and Health 42, 4159–4180.

Podolský, F., Ettler, V., Šebek, O., Ježek, J., Mihaljevič, M., Kříbek, B., Sracek, O., Vaněk, A., Penížek, V., Majer, V., Mapani, B., Kamona, F., Nyambe, I., 2015. Mercury in soil profiles from metal mining and smelting areas in Namibia and Zambia: distribution and potential sources. Journal of Soils and Sediments 15, 648–658.

Qiu, G.L., Feng, X.B., Wang, S.F., Shang, L.H., 2006. Environmental contamination of mercury from Hg-mining areas in Wuchuan, northeastern Guizhou, China. Environmental Pollution 142, 549–558.

Quintanilla-Villanueva, G.E., Villanueva-Rodríguez, M., Guzmán-Mar, J.L., Torres-Gaytan, D.E., Hernández-Ramírez, A., Orozco-Rivera, G., Hinojosa-Reyes, L., 2020. Mobility and speciation of mercury in soils from a mining zone in Villa Hidalgo, SLP, Mexico: a preliminary risk assessment. Applied Geochemistry 122, 104746.

Rahaman, M.S., Rahman, M.M., Mise, N., Sikder, M.T., Ichihara, G., Uddin, M.K., Kurasaki, M., Ichihara, S., 2021. Environmental arsenic exposure and its contribution to human diseases, toxicity mechanism and management. Environmental Pollution 289, 117940.

Raj, D., Kumar, A., Maiti, S.K., 2020. Mercury remediation potential of *Brassica juncea* (L.) Czern. for clean-up of flyash contaminated sites. Chemosphere 248, 125857.

Ramazanova, E., Lee, S.H., Lee, W., 2021. Stochastic risk assessment of urban soils contaminated by heavy metals in Kazakhstan. Science of the Total Environment 750, 141535.

Ran, H.Z., Guo, Z.H., Yi, L.W., Xiao, X.Y., Zhang, L., Hu, Z.H., Li, C. Z., Zhang, Y.X., 2021. Pollution characteristics and source identification of soil metal(loid)s at an abandoned arsenic-containing mine, China. Journal of Hazardous Materials 413, 125382.

Rehman, M.U., Khan, R., Khan, A., Qamar, W., Arafah, A., Ahmad, A., Ahmad, A., Akhter, R., Rinklebe, J., Ahmad, P., 2021. Fate of arsenic in living systems: Implications for sustainable and safe food chains. Journal of Hazardous Materials 417, 126050.

Ren, W., Duan, L., Zhu, Z.W., Du, W., An, Z.Y., Xu, L.J., Zhang, C., Zhuo, Y.Q., Chen, C.H., 2014. Mercury transformation and distribution across a polyvinyl chloride (PVC) production line in China. Environmental Science & Technology 48, 2321–2327.

Saiz-Lopez, A., Sitkiewicz, S.P., Roca-Sanjuán, D., Oliva-Enrich, J. M., Dávalos, J.Z., Notario, R., Jiskra, M., Xu, Y., Wang, F.Y., Thackray, C.P., Sunderland, E.M., Jacob, D.J., Travnikov, O., Cuevas, C.A., Acuna, A.U., Rivero, D., Plane, J.M.C., Kinnison, D.E., Sonke, J.E., 2018. Photoreduction of gaseous oxidized mercury changes global atmospheric mercury speciation, transport and deposition. Nature Communications 9, 4796.

Salmi, A., Boulila, F., 2021. Heavy metals multi-tolerant *Bradyrhizobium* isolated from mercury mining region in Algeria. Journal of Environmental Management 289, 112547.

Silva, V., Loredo, J., Fernández-Martínez, R., Larios, R., Ordóñez, A., Gómez, B., Rucandio, I., 2014. Arsenic partitioning among particle-size fractions of mine wastes and stream sediments from cinnabar mining districts. Environmental Geochemistry and Health 36, 831–843.

Singh, S., Kumar, V., Gupta, P., Singh, A., 2022. Conjoint application of novel bacterial isolates on dynamic changes in oxidative stress responses of axenic *Brassica juncea* L. in Hg-stress soils. Journal of Hazardous Materials 434, 128854.

Song, Z.C., Wang, C., Ding, L., Chen, M., Hu, Y., Li, P., Zhang, L.M., Feng, X.B., 2021. Soil mercury pollution caused by typical anthropogenic sources in China: Evidence from stable mercury isotope measurement and receptor model analysis. Journal of Cleaner Production 288, 125687.

Sun, H., Li, Y., Ji, Y., Yang, L., Wang, W., 2009. Spatial distribution and ecological significance of heavy metals in soils from Chatian Mercury Mining Deposit, Western Hunan province. Environmental Science 30, 1159–1165.

Tang, X.C., Wu, X.L., Xia, P.H., Lin, T., Huang, X.F., Zhang, Z.M., Zhang, J.C., 2021. Health risk assessment of heavy metals in soils and screening of accumulating plants around the Wanshan mercury mine in Northeast Guizhou Province, China. Environmental Science and Pollution Research 28, 48837–48850.

Tian, Z.J., Li, G.W., Tang, W.Z., Zhu, Q.H., Li, X.G., Du, C.L., Li, C. L., Li, J.X., Zhao, C., Zhang, L.Y., 2022. Role of *Sedum alfredii* and soil microbes in the remediation of ultra-high content heavy metals contaminated soil. Agriculture, Ecosystems & Environment 339, 108090.

Tomiyasu, T., Matsuyama, A., Imura, R., Kodamatani, H., Miyamoto, J., Kono, Y., Kocman, D., Kotnik, J., Fajon, V., Horvat, M., 2012. The distribution of total and methylmercury concentrations in soils near the Idrija mercury mine, Slovenia, and the dependence of the mercury concentrations on the chemical composition and organic carbon levels of the soil. Environmental Earth Sciences 65, 1309–1322.

Wang, L.W., Hou, D.Y., Cao, Y.N., Ok, Y.S., Tack, F.M.G., Rinklebe, J., O'Connor, D., 2020. Remediation of mercury contaminated soil, water, and air: A review of emerging materials and innovative technologies. Environment International 134, 105281.

Wang, S.X., Wang, J., Li, J.M., Hou, Y.N., Shi, L., Lian, C.L., Shen, Z.G., Chen, Y.H., 2021. Evaluation of biogas production potential of trace element-contaminated plants via anaerobic digestion. Ecotoxicology and Environmental Safety 208, 111598.

Wei, R.H., Chen, C., Kou, M., Liu, Z.Y., Wang, Z., Cai, J.X., Tan, W. F., 2023. Heavy metal concentrations in rice that meet safety standards can still pose a risk to human health. Communications Earth & Environment 4, 84.

Wei, S.H., Zhang, H., Tao, S.S., 2019. A review of arsenic exposure and lung cancer. Toxicology Research 8, 319–327.

Weiss-Penzias, P.S., Gay, D.A., Brigham, M.E., Parsons, M.T., Gustin, M.S., Schure, A.T., 2016. Trends in mercury wet deposition and mercury air concentrations across the U. S. and Canada. Science of the Total Environment 568, 546–556.

Wu, L.J., Yue, W.F., Wu, J., Cao, C.M., Liu, H., Teng, Y.G., 2023. Metal-mining-induced sediment pollution presents a potential ecological risk and threat to human health across China: A meta-analysis. Journal of Environmental Management 329, 117058.

Wu, Z.Y., Zhang, L.N., Xia, T.X., Jia, X.Y., Wang, S.J., 2020. Heavy metal pollution and human health risk assessment at mercury smelting sites in Wanshan district of Guizhou Province, China. RSC Advances 10, 23066–23079.

Xiao, X., Zhang, J.X., Wang, H., Han, X.X., Ma, J., Ma, Y., Luan, H. J., 2020. Distribution and health risk assessment of potentially toxic elements in soils around coal industrial areas: a global meta-analysis. Science of the Total Environment 713, 135292.

Xie, N., Kang, C., Ren, D.X., Zhang, L., 2022. Assessment of the variation of heavy metal pollutants in soil and crop plants through field and laboratory tests. Science of the Total Environment 811, 152343.

Xu, J.Y., Bravo, A.G., Lagerkvist, A., Bertilsson, S., Sjöblom, R., Kumpiene, J., 2015. Sources and remediation techniques for mercury contaminated soil. Environment International 74, 42–53.

Xu, X.H., Meng, B., Zhang, C., Feng, X.B., Gu, C.H., Guo, J.Y., Bishop, K., Xu, Z.D., Zhang, S.S., Qiu, G.L., 2017. The local impact of a coal-fired power plant on inorganic mercury and methyl-mercury distribution in rice (*Oryza sativa* L.). Environmental Pollution 223, 11–18.

Xu, Z.D., Lu, Q.H., Xu, X.H., Feng, X.B., Liang, L.C., Liu, L., Li, C., Chen, Z., Qiu, G.L., 2020. Multi-pathway mercury health risk assessment, categorization and prioritization in an abandoned mercury mining area: A pilot study for implementation of the Minamata Convention. Chemosphere 260, 127582.

Xun, Y., Feng, L., Li, Y.D., Dong, H.C., 2017. Mercury accumulation plant *Cyrtomium macrophyllum* and its potential for phytoremediation of mercury polluted sites. Chemosphere 189, 161–170.

Yang, J.Z., Sun, Y.L., Wang, Z.L., Gong, J.J., Gao, J.W., Tang, S.X., Ma, S.M., Duan, Z., 2022. Heavy metal pollution in agricultural soils of a typical volcanic area: Risk assessment and source appointment. Chemosphere 304, 135340.

Yang, S.Y., Gu, S.B., He, M.J., Tang, X.J., Ma, L.Q., Xu, J.M., Liu, X.M., 2020. Policy adjustment impacts Cd, Cu, Ni, Pb and Zn contamination in soils around e-waste area: Concentrations, sources and health risks. Science of the Total Environment 741, 140442.

Yin, D.L., He, T.R., Yin, R.S., Zeng, L.X., 2018. Effects of soil properties on production and bioaccumulation of methylmercury in rice paddies at a mercury mining area, China. Journal of Environmental Sciences 68, 194–205.

Yuan, X.H., Xue, N.D., Han, Z.G., 2021. A meta-analysis of heavy metals pollution in farmland and urban soils in China over the past 20 years. Journal of Environmental Sciences 101, 217–226.

Zeng, J., Han, G.L., Zhang, S.T., Liang, B., Qu, R., Liu, M., Liu, J.K., 2022. Potentially toxic elements in cascade dams-influenced river originated from Tibetan Plateau. Environmental Research 208, 112716.

Zeng, Q.B., Zou, Z.L., Wang, Q.L., Sun, B.F., Liu, Y.L., Liang, B., Liu, Q.Z., Zhang, A.H., 2019. Association and risk of five miRNAs with arsenic-induced multiorgan damage. Science of the Total Environment 680, 1–9.

Zhang, X.H., Tian, K., Wang, Y.M., Hu, W.Y., Liu, B.L., Yuan, X.Y., Huang, B., Wu, L.H., 2023. Identification of sources and their potential health risk of potential toxic elements in soils from a mercury-thallium polymetallic mining area in Southwest China: Insight from mercury isotopes and PMF model. Science of the Total Environment 869, 161774.

Zhao, Z.J., Hao, M., Li, Y.L., Li, S.H., 2022. Contamination, sources and health risks of toxic elements in soils of karstic urban parks based on Monte Carlo simulation combined with a receptor model. Science of the Total Environment 839, 156223.